

Protein purification to analyze AAA+ proteolytic machine in vitro

Diego Rojas

Department of Biological Sciences, Columbia University, New York, USA

The ATP-dependent ClpXP protease of *Escherichia coli* consists of two subunits, the ClpP subunit, which has the proteolytic activity and the AAA⁺ motor ClpX, which mechanically unfolds and translocates substrates for ClpP degradation. In order to investigate the mechanical properties of ClpXP during substrate unfolding using magnetical tweezers, here we optimize protocols to purify ClpP and a model substrate based on human Filamin A from *E. coli* lysates by a combination of metal affinity chromatography and fast performance liquid chromatography (FPLC). ClpX purification was challenging and remains to be improved. Importantly, a HaloTag protein molecule was fused to the Filamin substrate, which allowed covalent bonding to surfaces or fluorescent molecules. We analyzed the mechanical properties of a single Filamin A substrate using atomic force spectroscopy (AFM) and found good correlation with previous single-molecule experiments based on optical tweezers. AFM experiments also demonstrate the successful binding of the HaloTag moiety to a modified glass surface. The results show that the study of ClpXP-mediated degradation of proteins by magnetic tweezers has the potential to unveil the mechanics of protein degradation inside cells.

Physiological functions of protein degradation

In order to respond to external stress and developmental signals, a cell needs to adjust the availability and activity of proteins, especially key metabolic enzymes and regulatory proteins [1]. Protein activity is under the control of several well-known mechanisms, including changes in localization, reversible covalent modifications, interactions with small molecule effectors and other proteins, transcriptional and translational regulation synthesis, among others [1, 2]. Intracellular proteins are also regulated by proteolysis, a key process that plays a role in modulating the levels of metabolic enzymes and removing anomalous and malfunctioning proteins from cells. In this regard, proteolysis could be seen as a drastic solution since restoration of the activity requires synthesis of a complete protein [1]. In general, all intracellular proteins from well-studied eukaryotic or prokaryotic organisms are continuously being degraded to amino acids. This process provides several evolutionary advantages to a cell and there are some principles that appear to favor the use of proteolysis as a regulatory mechanism rather than other alternatives.

First, due to the fact that many errors may occur during protein translation, proteolysis jettisons defective proteins whose accumulation could trigger cell aging and/or death [3].

Second, even when most proteins are relatively stable in vivo, a subset of carefully regulated proteins has very short half-lives. Since these short lived proteins are present in limiting amounts, they will be rapidly responsive to changes in their rate of synthesis and/or degradation. In fact, the stability of proteins is highly correlated with the mRNAs that encode them. If an mRNA or its product were totally stable, they would theoretically accumulate to dangerous concentrations [2]. In contrast, if new synthesis of an unstable protein is not continuous but is restricted to specific biological stages, loss of the activity of unstable protein would provide an effective checkpoint control for its production.

Third, even when widely used mechanisms like phosphorylation or reversible modification provide alternatives for inactivating proteins, proteolysis seems to provide more advantages in developmental pathways in which unstable proteins play a role during a limited period [1]. In this case, there is no particular advantage to a reversal modification since the protein will not be needed again. In contrast, loss of the protein may be important to avoid potentially damaging activity under the different conditions. For example, modulation of proteolytic activity may affect the development of adipose tissue, and malfunctioning of this process may produce several disorders like obesity, diabetes, atherosclerosis, among others [4]. Therefore, proteolysis helps to maintain cellular homeostasis by removing not only short lived regulatory proteins, but also proteins that are misfolded and damaged.

ClpP

Protein degradation in the cell is mainly carried out by oligomeric, cylindrical, self-compartmentalized, energy dependent proteases [5]. Among these enzymes, Caseinolytic protease (ClpP) is a well-studied member of the ATP-dependent serine-type Clp family. Excepting archaea, mollicutes and some fungi, ClpP is a highly conserved serine protease present through bacteria and eukaryota [6]. It was discovered in *Escherichia coli* by Katayama-Fujimura and co-workers [7], and to date, ClpP structures have been solved from five different organisms, including *E. coli*, *Streptococcus pneumoniae*,

Plasmodium falciparum, *Mycobacterium tuberculosis* and *Homo sapiens*, and all of them share a high degree of similarity [6].

Among these structures, it was found that the ClpP cylinder maintains the same overall assembly and construction, and the variations are present in the core ClpP structure to provide specific functions that allow organisms to adapt to diverse cellular environments [8]. For instance, the X-ray structure of ClpP from *E. coli* shows a cylindrical-shaped tetradecamer of about 300 kDa in molecular weight and 90 Å in both diameter and height. Each ClpP subunit has six repeats of α/β -fold ($\alpha A/\beta 1/\beta 2$, $\alpha B/\beta 3/\beta 4$, $\alpha C/\beta 5/\beta 6$, $\alpha D/\beta 7/\beta 8$, $\alpha F/\beta 10$, and $\alpha G/\beta 11$) with an additional $\alpha\beta$ unit (E/9) [8]. These subunits are held together mainly by hydrophobic interactions to form the homotetradecameric complex consisting of two stacked heptameric rings with the active sites enclosed within the equatorial chamber [8, 9]. Each subunit can be divided into a handle region that mediates ring-ring interaction, and a head domain. Similarly, each heptameric ring is made from the packing of head domains, exposing 7 handle regions which intercalate with the correspondent seven head regions of the second heptameric ring, creating a tetradecamer with a spherical internal chamber [6, 8]. Although the handle region is the only area where two ClpP rings have contact, the physical interactions in this region together with charge-charge interaction networks among the head domains held both rings associated, indicating a high degree of plasticity in this region. Access to this cavity is mediated by narrow axial entrance pores [6, 8].

ClpP is first synthesized as a 207-residue protein including an N-terminal sequence which acts as a regulatory peptide and undergoes autoproteolysis to generate a mature ClpP of 193-amino acids [9]. In *E. coli*, ClpP associates with the AAA⁺ (ATPases Associated with diverse cellular Activities) chaperones ClpX and ClpA, well studied members of the Clp/Hsp100 family [6, 9]. Native ClpP has a limited serine-peptidase activity against peptides with less than 6 residues, cleaving them after hydrophobic residues. Moreover, degradation of peptides longer than 6 residues requires the activity of an ATPase subunit such as ClpA to form the active protease ClpAP, but not ATP hydrolysis. In contrast, degradation of protein substrates requires both ATP hydrolysis and the cooperation of ATP-driven chaperones [9]. Protein substrates are cleaved in a highly processive manner, generating 7 to 10 residue peptides, but the pattern of degradation does not have any sequence specificity. Furthermore, the chaperones recognize specific substrates with or without the presence of adaptors, unfold these substrates and translocate them into the proteolytic core of ClpP for degradation [8].

On the apical surface of ClpP, there are seven grooves of about 10 Å in diameter mainly composed by conserved hydrophobic residues that provide pockets for specific loop regions present in the structure of the chaperones [8]. These loop regions are highly conserved in ClpX and other AAA⁺ chaperones that bind to ClpP. Therefore, the chaperone-protease interaction is mediated by loop-groove interactions instead of interactions between large surfaces [9]. This kind of interaction would circumvent the symmetry mismatch that exists between ClpP, which has seven-fold symmetry, and ClpX, which has six-fold symmetry [10]. However, it is not known whether the mismatch between ClpX hexamer and ClpP oligomer is an evolutionary result to allow the rings to rotate about each other, improving the rate of translocation of unfolded substrates. This loop-groove interaction seems to provide the chaperone-protease complex with more structural flexibility, serving as a lubrication device to facilitate relative rotation. Because the primary interaction between the two rings takes place at a single site, it is easier to disrupt than if the same interaction involves six or seven sites around the ring [10]. In other words, the symmetry mismatch may serve as a quick release mechanism, facilitating the separation between the ATPase and the protease in order to bind different interaction molecules or multiple substrates [10].

ClpX

ATP-dependent proteases like ClpP must select out abnormal proteins and specific proteins whose activities are regulated by degradation from the bulk of cytoplasmic proteins. This means that there must be some degree of specificity in recognition of targets [11]. This is the case of ClpP dependent proteases, whose substrate specificity is determined by the type of ATPase component, ClpA or ClpX, partners with ClpP. By itself, ClpP degrades only short polypeptides in an ATP-dependent reaction [11]. However, larger polypeptides can be hydrolyzed if ClpP is associated with these chaperones. The biological functions of ClpX include protein unfolding, polypeptide translocation, and binding substrates, adaptors, and/or ClpP [12]. Both unfolding and translocation require ATP binding and hydrolysis to catalyze the enzyme conformational changes needed during these mechanical processes. Furthermore, ATP binding but not hydrolysis is required for binding ClpX to ClpP [13].

Subunits of ClpX contain a family of specific N-terminal domains and large and small AAA⁺ domains [12]. These domains function together in hexameric rings, forming a cleft where ATP or ADP binds. This cleft is mainly formed by conserved sequence motifs that define the AAA⁺ superfamily [12]. However, variants lacking the N-domain

(ClpX^{AN}) can still combine with ClpP to mediate efficient degradation of native *ssrA*-tagged proteins [12, 14]. Interestingly, ClpX^{AN} binds ClpP with similar wild-type affinity and supports ATP-dependent degradation of several native protein substrates at rates near to wild-type ClpXP, demonstrating that the AAA⁺ domains perform the mechanical functions of ClpX [12].

The crystal structure reveals asymmetry in ring hexamers of nucleotide-free and nucleotide-bound ClpX [12]. Asymmetry arises from large changes in rotation between the large and small AAA⁺ domains of individual subunits. This difference generates a mechanism for coupling conformational changes generated by ATP binding or hydrolysis in one subunit to flexing motions of the ring [12]. The axial pore of the ClpX hexamer serves as the translocation channel into ClpP. Furthermore, three different pore loops called GYVG, pore-2, and RKH play roles in binding the *ssrA* tag and also mediate binding to and communication with ClpP and are needed for protein unfolding and translocation [12]. Degradation is initiated when these loops engage an unstructured region of a protein substrate. ATP-fueled conformational changes in the ring may produce pulses of pulling that unfold the protein substrate and translocate it through the pore and into the degradation chamber of ClpP [15].

ClpXP

Electron micrographs of negatively stained ClpXP preparations initially showed side complexes in which ClpP was flanked on either one or both sides by a ring of ClpX [11]. In these complexes, the axial pores of the ClpX rings align with the pores in the ClpP rings, facilitating the movement of substrates through the chamber. Apparently, in doubly-capped ClpX-ClpP-ClpX complexes, translocations occur in only one of the two ClpX rings, indicating a coordinated system between both ClpX rings and ClpP [16].

As noted above, a ClpX ring has six subunits and a ClpP ring has seven subunits, making a symmetry mismatch mandatory. This complex appears to be stabilized by a group of interactions involving the loops near the axial pores of each ring, and another group between peripheral structural elements in the ClpX and ClpP rings [16]. Specifically, the peripheral ClpXP interactions involve a coupling between the conserved sequences in surface ClpX loops with clefts on the faces of the ClpP ring. This tight binding of ClpX to ClpP requires ATP and is enhanced moderately during substrate degradation. Furthermore, ATP binding seems to trigger conformational changes in ClpX that allow it to bind to the ClpP surface [17].

In the ClpXP complex, ClpX recognizes unstructured peptide sequences in its protein substrates, and unfolds

the stable tertiary structure of protein substrates into the chamber of ClpP for degradation. Substrates are recognized by short peptide sequences such as the *ssrA* tag, which mediates the initial binding of the substrate to the loops within the axial pore of the ClpX ring [18].

Single molecule approaches to study biological molecules

Previous studies of protein degradation machines have been based on the analysis of dynamics of substrate denaturation or translocation by measuring the average of large populations of enzymes and substrates. However, specific molecular mechanisms used by proteases cannot be assessed by these approaches. In contrast, single molecule experiments can answer important questions about the mechanical properties of several proteins. For instance, single-molecule force spectroscopy has emerged as a reliable tool to investigate the forces and mechanical behavior associated with enzymes and other biological molecules.

The ability to accurately measure mechanical forces is essential to understand the conformational dynamics of proteins under the stretching generated by an external force with Angstrom resolution [19]. For several years, mechanical manipulations at the single molecule level of proteins were restricted to atomic force microscopy (AFM) techniques [19]. However, these techniques cannot work properly with proteins that exhibit a relatively high degree of mechanical stability because they require long unfolding times that AFM techniques are not allowed to make [20]. For example, ClpXP protease has been studied by optical tweezers to analyze the mechanics of enzymatic unfolding and translocation of single molecules of a substrate. ClpXP was attached to one polystyrene bead, a multidomain substrate was tethered to a second bead using a double-stranded DNA, and the beads were connected by interactions between ClpXP and substrate. By using this set-up, Aubin-Tam and co-workers [15] were able, not only to probe the ability of ClpX to perform mechanical work, but also, to propose a power-stroke model of denaturation mediated by ClpXP. However, this technology has important limitations and drawbacks that difficult its application. For instance, manipulating a protein with optical tweezers relies on the ability to attach the protein to long DNA linker. Unfortunately, the streptavidin-biotin unbinding force used in the attachment of the DNA linkers with the polystyrene bead is usually lower than the then the unfolding forces, limiting to study proteins with low mechanical stability [19]. In contrast, magnetic tweezers allow the manipulation of single molecules tethered to magnetic beads located inside a magnetic field, generating stretching forces of a few tens of pN.

HaloTag

There is an increasing necessity for scientists to develop protocols that allow them to study specific cellular and molecular mechanisms. Many of these methods rely on the manipulation of molecules for selective protein visualization, capture, and manipulation. Many of these manipulations imply the use of tag proteins and peptides, which often requires the use of more than one tag and therefore, multiple genetic constructions. In this regard, HaloTag allows meeting several needs of different experimental procedures [21].

The HaloTag approach is based on a modular protein tag which has a haloalkane dehalogenase capable of bonding efficiently with haloalkanes by removing halides from aliphatic hydrocarbons, and a chloroalkane linker which forms stable bonds with synthetic molecules. In this way, a covalent bond is formed between the HaloTag protein and a synthetic ligand [21]. This covalent union enables irreversible attachment of the HaloTag protein to surfaces or the stable linking of tags for visualizing this protein. As a result, this technology allows specific fluorescent labeling of proteins fused the Halotag protein as well as irreversible capture of these proteins onto solid supports [21].

The breakthrough of HaloTag lies in the use of a cDNA encoding a non-fluorescent protein fusion instead of a gene for a fluorescent protein like GFP. Therefore, HaloTag proteins can be fused with the protein of interest, creating a chimeric protein that will be expressed as monomers. This construct provides to advantages for scientist studying a protein or cellular process [21, 22]. First, the HaloTag protein interacts with a HaloTag ligand containing biotin that can be used to capture the protein of interest. Second, incubating the protein fused with the HaloTag protein, together with a HaloTag ligand which possesses a reporter group like a fluorophore, will result in the detection by fluorescence. Therefore, this technology gives plasticity for both, the purification and detection of the protein of interest [21, 22].

Filamin

Filamin is a high molecular weight protein that was purified from rabbit macrophages and then, isolated from chicken gizzard smooth muscle [23, 24]. This protein is part of the intracellular filamentous structure of several types of cells and has a broad phylogenetic distribution [25]. The filamin family is composed by three homologous proteins called FLNA, FLNB and FLNC, which are the product of different genes and their mRNA splice products. Filamin A and B are the most broadly expressed isoforms; however, the level of expression of filamin B is

different in each tissue. Given the ubiquitous functions of filamins during cell motility and signaling, mutations in these genes could be involved in a wide spectrum of physiological disorders [25]. In fact, mutations in FLNA are known to be related with congenital and developmental malformations of the bone, brain, limbs, and heart in humans [26]. Because its role in cell mechanics by myosin contraction, FLNA has been subject to several studies in order to elucidate the mechanical properties by using magnetical tweezers or AFM [25, 27]. Filamin A is a dimeric protein composed by two subunits of 280-kDA. Each subunit has an N-terminal actin-binding domain followed by 24 immunoglobulin (Ig) repeats separated in three segments by two molecular hinges. The first segment, rod 1, is composed by repeats 1-15 in an extended linear array. Rod 2 (repeats 16-23) is more compact and is implicated in the sensitivity of filamin to mediate mechanical forces in cells, whereas the third segment is composed by repeat 24.

Filamin has been used to study protein unfolding and translocation by ClpXP using optical tweezers. The construct, as shown in figure 2A,, has three main components. First, it has eight filamin A domains, that provide measurements of protein unfolding as ClpX produces mechanical force to translocate the substrate into the lumen of ClpP. Second, a HaloTag domain attached to the N-terminus of the filamin A domains, that allows not only to bind covalently this substrate to a glass surface for its analysis using optical tweezers, but also, to attach fluorescent tags that are used to observe substrates containing tag molecules in SDS-PAGE. Finally, it has an ssr-A tag that is used of the recognition of this substrate by ClpX.

In order to study ClpXP protease using magnetic tweezers, it is necessary a high purity of the proteins being used to measure the activity of single molecules. To this end, we optimized protocols for purification of Filamin and ClpP. Moreover, we analyzed the mechanical properties of a single Filamin A substrate using atomic force spectroscopy (AFM) to study the unfolding properties of this substrate when is attached to a HaloTag protein. Mechanical unfolding experiments of filamin A are in principle equivalent to the ClpXP-induced unfolding of this protein substrate. Therefore, the results of filamin unfolding using AFM can be a reference to investigate, using magnetic tweezers, the dynamics of ClpX as it encounters a folder substrate such as filamin and translocates it through the ClpP processing pore.

RESULTS

Protein purification

When ClpX was expressed for the first time, we observed protein precipitation. Therefore, it was necessary to

prepare buffers with 10% glycerol in order to circumvent this problem. However, after expressing ClpX under the strong T7 promoter, only a small portion was found in the soluble portions of cell extracts, and the remainder was found in the pellet. In order to increase the production of this protein, we had to increase up to ten-fold the volume of culture, use Ammonium Sulfate (0.4g/mL) to induce protein precipitation, use Hepes instead of Tris-buffer, and change DTT for TCEP. Unfortunately, the band corresponding to ClpX in the SDS-PAGE did not seem to correspond to the actual ClpX (Adrian O. Olivares, personal communication) (figure 1A). Therefore, the ClpX protein we used in this study was given by Adrian O. Olivares (Massachusetts Institute of Technology, Cambridge, MA).

The Western Blot analysis of the pilot expression of ClpX shows that the fractions obtained by the Superdex 200HR column do not contain ClpX. Moreover, the time used to express ClpX affects not only the final concentration of this protein, but also, is correlated with degradation of ClpX. When ClpX was expressed during 2 or 3 hrs, the band observed was weak, showing a low expression of this protein (figure 3C). However, after 4 hrs, the expression seems to increase as well as the number of bands observed in each sample, an indication that ClpX becomes degraded over the time of protein expression.

For ClpP and filamin, the main protein fraction was observed in the soluble portion of the cell lysate, which is consistent with the higher peaks observed in the chromatograms (Figure 1B and 1C). To optimize the yield of the purification of ClpP, several buffers were tried. With these improvements together with the increase in the volume of cell culture used, we were able to increase 25 times the final concentration of this enzyme. In order to increase the yield of filamin production, we tried to express it overnight at 25°C but the result was negative and the observed chromatogram showed several peaks, indicating a non-pure product that could not be used for further experiments (figure 1C). The final weight of the pellet from the cellular extracts was approximately 1.85, 1.93 and 2.08 grams for ClpX, ClpP and filamin respectively.

Purified ClpP in fractions from Superdex 200HR column coincided with the appearance of a protein with an apparent M_r of 23 kDa as determined by SDS-PAGE. This result agreed with that reported by Maurizi *et al.* [5]. In the case of ClpX, we observed a protein with a M_r of 260 kDa, which differs from the 240 kDa protein obtained by Aubin-Tam [15]. For filamin, we obtained a band corresponding to 140 kDa, which is consistent with the results obtained by Furuike *et al.* [27] (figure 1C).

Filamin unfolding

We analyzed extension of filamin A using AFM. When filamin was pulled at constant velocity, the pulling force initiated the unfolding of a FLN module or the HaloTag protein. In this case, there were nine peaks corresponding to the unfolding of the eight FLN modules and the HaloTag protein, which were 32 nm and 66 nm respectively (Figure 2A). When the pulling force was done under a feedback system that maintained a constant force, a stair-like elongation, composed by nine steps was observed (figure 2B). Similarly, unfolding probability of the multidomain substrate increased when higher forces were applied to pull this molecule (figure 2C). Similarly, force-dependent rate results during mechanical unfolding (AFM) corresponded to those obtained for ClpX unfolding using optical-trapping nanometry [15] (figure 2D).

Filamin degradation

First, we tested the ability of filamin as a substrate of ClpXP due the presence of the HaloTag and the *ssrA*-tag in its structure. As shown in figure 3C, only the fragments derived from the FLN polypeptide were visible under UV light ($\lambda=590$ nm). In this case, the attachment of Coumarin tag to the HaloTag protein allowed the detection of these fragments. Second, the confirmed ClpXP activity was defined as the ability to degrade filamin *in vitro* in an ATP-dependent reaction. As observed in figure 3A, the smaller fragment represents a product of filamin degradation that also contains the HaloTag, showing that the protease activity of ClpXP is conserved after the purification.

In the presence of ATP, ClpXP promoted the degradation of purified filamin protein (figures 3A and 3B), which contains the *ssrA*-tag and has been shown to be a specific substrate for ClpX and ClpP *in vitro*. The chromatograms of ClpP isolated from cell extracts on SH column was very similar to that described by these proteins elsewhere [11].

To investigate single molecule activity, we attached a complex of ClpXP and filamin between a fluorescent bead and a glass cover. As shown in figure 4, the substrate – composed by eight repeats immunoglobulin like domains – contains an N-terminal HaloTag that tethers the molecule to the fluorescent bead and an *ssrA*-tag that to target it to ClpXP. Similarly, the biotin molecule was added by the BirA enzyme in the ClpX structure. Biotin was used to attach ClpXP to a streptavidin-coated glass. Our experimental set-up, consisting of a combination of the TIRF microscope, a camera photon-multiplier, and an electromagnetic head located on top of the microscope. During the experiment, when a magnetic field is applied, a fraction of the beads remain tethered to the surface. In the best case scenario, a single polypeptide on the surface of one of the beads starts being unfolded and

translocated by the ClpX AAA⁺ motor in the presence of ATP. Figure 5 shows a trace where a filamin domain is unfolded and translocated forward and backward. When ClpP is added to the solution, in some instances it forms a complex with ClpX, creating the ClpXP machine and the translocated substrates become degraded. So far, we obtained only a few traces with events that may correspond to unfolding –translocation events (see figure 6 for an example). When ClpX unfolds a FLN domain, the protein backbone is extended by the force of the bead. Then, ClpX starts working against this force and translocates the protein toward degradation. A second larger unfolding step is seen for HaloTag, which similarly to FLN, is translocated and degraded.

In our results, we observed two distinct behaviors of ClpXP degradation of single substrate molecules. In one case, ClpXP was able to unfold and translocate one domain of the substrate but was not able to degrade it (figure 5). In contrast, figure 6 shows the events related to ClpXP unfolding, translocation and degradation of filamin domains of the substrate. Unfolding of one filamin residue resulted in 4-6 nm increases in bead separation whereas translocation of domains produced a shortening of approximately 7nm.

The filamin-HaloTag construct combined with the coumarin ligand yielded a fluorescent product that was stable under the denaturing conditions for SDS-PAGE analysis (0.1% SDS; 100°C, 10 min). Formation of a stable covalent bond between filamin-HaloTag and the glass surface was evident when it was stretched using AFM. This bond allowed us to generate forces up to 200 pN to the substrate.

DISCUSSION

To explore the role of ClpXP protease in the biological regulation of several cellular functions and pathways, it is necessary to obtain ClpX and ClpP free of proteins that could interfere with their activity in vitro during magnetic tweezers experiments. The elution profiles of filamin and ClpP are highly reproducible. In addition, once standardized, the procedures described above are relatively simple and could be completed within four days.

The purity of the isolated proteins assessed by SDS-PAGE analysis (figures 1) shows the absence of other well defined bands, which is a proof of biochemical purity. Moreover, the fact that the multidomain substrate was degraded shows that functional activities of ClpX and ClpP were conserved. Although the trace corresponding to successful substrate unfolding, most of our recordings showed frequent slippage events (figure 5), in which ClpX seemed to fail in unfolding the domain, releasing the substrate, and moving in a backward trajectory along the

substrate. This result is similar to previous degradation studies showing that stable substrates with a short ssrA-tag are frequently released and refolded by ClpXP before successful unfolding [28, 29]. In any case, the single-molecule unfolding and translocation recordings were not unambiguous and ClpXP did not show a reproducible degradation of substrate. Similarly, some traces seemed to show ClpXP behavior, although no conclusive or reproducible.

Even though the difficulties observed during ClpX purification, the pilot expression of this protein observed by western blot, allowed us to comprehend that the possible error in our procedure stems in the time used for expressing ClpX. In this case, our future improvements will be focused not in the augmentation of the volume of cell culture used, but in the extension of the expression period. However, as shown in figure 3C, as the time of ClpX expression is extended, degradation of the protein seems to follow this process. Therefore, we need to standardize the time in which ClpX will be expressed.

In this study, filamin with a HaloTag protein attached to its N-terminus was used. The resulting chimera was suitable for being studied for ClpXP degradation, magnetical tweezers and AFM. This feature is very important because the HaloTag protein did not affect the functionality of filamin and possibly, its structure. The HaloTag technology served as a detection system for labeled filamin substrates. This approach is based on the covalent bond between the HaloTag protein and the synthetic ligand, in this case, Coumarin. This interaction is very stable and was maintained after conditions expected to disrupt protein conformation such as boiling in SDS. Furthermore, after irradiation of the samples with UV light ($\lambda=590$ nm), only substrates with Coumarin attached are detected, and we were able to observe not only intact filamin, but sub-products of degradation. Similarly, we were able to analyze mechanical unfolding of filamin A generating forces up to 150 pN. This shows high mechanical stability of FLN A.

Although the understanding of the motor properties of ClpXP are far from the scope of this study, these results serve to set the basis of the application of magnetical tweezers in the study of this protease. Furthermore, magnetic tweezers offer some advantages over other force spectroscopy techniques like low force range and resembles in vivo conditions. This technique is an appropriate approach to study the behavior of mechanically stable proteins in the low-force regime, providing an ideal tool for studying ClpXP for long periods, complementing the data obtained by AFM. Future development in the purification of ClpX, and the manipulation of ClpXP and filamin with magnetic tweezers will allow us to understand the motor

mechanisms of ClpXP used to degrade substrates with different molecular stabilities.

We found that the force required to unfold the HaloTag domain was higher than the one needed to unfold a FLN domain. Each FLN unfolding required a force of approximately 100 pN. This force was enough to extend each domain 25 nm. However, the extent of substrate elongation was larger when the HaloTag domain was unfolded compared to the domain extension of a single filamin domain. The mechanical stability of FLN A in our experiments is similar to those obtained from ClpX unfolding. The reported rates for unfolding filamin by ClpX are in accordance to those obtained with AFM if the force is 65 and 85 pN respectively [15].

In conclusion, FPLC presents the advantage of rapid isolation of ClpP and filamin proteins. Similarly, HaloTag allows the visualization of the substrate by SDS-PAGE and the attaching of the protein under study to be subject to stretching forces using AFM or magnetic tweezers. The final purpose of this study is to improve a method of protein purification that allows us to preserve the functional activity of the molecules analyzed by magnetic tweezers. It is possible that adjustments in the isolation of ClpX, preparations of glass cover slips as well as in the improvement in the mechanical manipulation of single proteins will eventually allow the reproducibility of the analysis of ClpXP protease using magnetic tweezers for studying the mechanical properties of substrates in the activity of this key molecular machine.

METHODS

Buffers

TBS contained 50 mM Tris (pH 8.0), and 150 mM NaCl. Lysis buffer contained 20 mM Hepes (pH 8.0), 10 mM imidazole, 400 mM NaCl, 100 mM KCl, 10% glycerol, and 10 mM β -mercaptoethanol. Elution buffer contained 20 mM Tris (pH 8.0), 250 mM imidazole, 400 mM NaCl, 100 mM KCl, 10% glycerol, and 10 mM β -mercaptoethanol. Biotinylation buffer contained 50 mM bicine (pH 8.3), 300 mM K^+ glutamate, 10% glycerol, 0.5 mM TCEP, and 0.05% NP40. Reaction buffer contained 4 mM ATP, 5 mM Magnesium Acetate, 1 mM biotin, and 1 μ M BirA. S300 buffer contained 20 mM Hepes (pH 7.6), 300 mM KCl, 0.1 mM EDTA, 10% glycerol, and 1 mM TCEP. W buffer (pH 7.3) contained 50 mM Sodium Phosphate, 300 mM NaCl, 10 mM β -mercaptoethanol and 20 mM imidazole. E Buffer (pH 7.1) contained 50 mM Sodium Phosphate, 300 mM NaCl, 10 mM β -mercaptoethanol, and 250 mM imidazole [15]. PD buffer (pH 7.6) contained 25 mM Hepes, 100 mM KCl, 10 mM $MgCl_2$, 10% glycerol, 0.1% tween-20, 10 μ M Coumarin and 100 mM DTT. S buffer (pH 8.0) contained 50 mM Phosium Phosphate, 1 M NaCl,

5 mM imidazole, and 10% glycerol. G1 buffer (pH 8.0) contained 50 mM Sodium Phosphate, 1 M NaCl, 10% glycerol, and 20 mM imidazole. G2 buffer was the same G1 buffer but contained 500 mM imidazole. Q buffer (pH 8.0) contained 50 mM Tris, 5mM DTT, 10mM $MgCl_2$, 10% glycerol, and 50 mM KCl; Q2 buffer was the same but contained 1 M KCl [13]. Clp buffer (pH 7.5) contained 50 mM Tris-HCl, 200 mM KCl, 25 mM $MgCl_2$, 1 mM DTT, 0.1 mM EDTA, and 10% glycerol. Borax buffer (pH 8.5) contained 100 mM of borax. PB buffer (pH 8.5) contained 150 mM Sodium Phosphate dibasic, and 50 mM ethanolamine. BB buffer (pH 8.5) contained 5mg/mL of NHS-PEG4-Biotin (Thermo Fisher Scientific) dissolved in Borax Buffer. Streptavidin buffer (pH 8.5) contained 150 mM of Sodium Phosphate dibasic, and 1mg/mL of Streptavidin. LB media (pH 7.0) contained 1% Tryptone, 1% NaCl, and 0.5% yeast extract. 1.5X YT broth (pH 7.0) contained 1.3% Tryptone, 0.75% yeast extract, and 0.75% NaCl.

Protein Expression and Purification

Enzymes and substrates were expressed using IPTG-inducible T7 promoters.

ClpX

Biotinylated ClpX^{SC}, a single-chain variant containing an N-terminal FLAG tag, six repeats of *E. coli* ClpX- Δ N (residues 61–423) connected by flexible linkers [30, 31], a BirA-acceptor peptide HAAGGLNDIFEAQKIEWHEDT [32]), and a C-terminal H₆ tag. ClpX^{SC} was expressed from a pACYC-derived vector in *E. coli* strain ERL (ER2566 with a chromosomal λ -lysozyme gene; a gift from Adrian O. Olivares, Massachusetts Institute of Technology, Cambridge, MA). The BirA enzyme contained a C-terminal H₆ tag and was expressed in strain BLR from a pET22 vector (a gift from Tania A. Baker, Massachusetts Institute of Technology, Cambridge, MA, USA). Cells were grown to OD₆₀₀ at 37°C in 1L of 1.5X YT broth with kanamycin (30 μ g/mL) and chloramphenicol (34 μ g/mL) chilled to 25°C, and induced with 1 mM IPTG. Cells were harvested 3 hr later, resuspended in TBS, and frozen at -80°C until purification. For protein extraction, cells were thawed and resuspended and lysed using lysis buffer, protease inhibitors (100 mM AEBSF, HCl; Calbiochem®), 1% Triton X-100, DNase I (Roche Applied Science®), RNase A (Roche Applied Science®) and $MgCl_2$. To improve cell lysis, samples were sonicated in ice bath (10 passes of 15 s) with a 5.0 mm probe sonicator followed by French Press (15,000 PSI). Insoluble debris was removed from the samples by centrifugation at 18,100 rpm for 40 min at 4°C. The supernatants were filtered using a 0.45 μ m filter and stored at -80°C. For purification, the lysates were thawed at 42°C and resuspended in lysis buffer. This

sample was mixed with equilibrated nickel-NTA resin during 1 hr at 4°C, lysates were centrifuged at 3,000 rpm for 7 min, and the clarified lysates were passed through a Ni²⁺-NTA affinity column (QIAGEN). After washing, bound proteins were eluted with elution buffer and the OD₂₈₀ of the fractions was analyzed using a spectrophotometer (Beckman Du® 620B). All the appropriate fractions with protein were pooled and dialyzed 3 hrs against 500 mL of Biotinylation buffer. After dialysis, reaction buffer was combined with the protein and 2 µM of BirA during 1 hr at 30°C. In these conditions, BirA catalyzes the biotinylation of ClpX^{SC} at the BirA-acceptor peptide. Samples were loaded onto a Superdex 200HRcolumn (GE Bio-Sciences, Piscataway, NJ) and equilibrated with S300 buffer. Chromatography was performed at 0.25 mL/min, and fractions of 250 µL were collected. All experiments were performed at 4°C. After chromatography, fractions were assayed by SDS-PAGE 10%.

ClpP

E. coli ClpP-H₆ was expressed in DH5α/pYK133/pRep4 (a gift from Tania A. Baker, Massachusetts Institute of Technology, Cambridge, MA, USA). Cultures were grown at 30°C to an OD₆₀₀ of 0.5 in 400 mL of LB containing carbenicillin (50 µg/mL) and kanamycin (30 µg/mL). IPTG was added to a final concentration of 0.5 mM and expression was conducted during 3 hr at 30°C. Cells were harvested by centrifugation and resuspended in S buffer. Cell lysis was the same used to extract ClpX but without the addition of protease inhibitors. The lysate was centrifuged for 20 min at 17,000 x g and the supernatant was added to 2 mL nickel-NTA resin (QIAGEN) previously equilibrated with S buffer. After rocking for 1 hr at 4°C, the resin was packed into a column and washed with S buffer and G1 buffer. ClpP was eluted with G2 buffer, and fractions containing protein were pooled in one single sample that was loaded onto a Superdex 200HRcolumn (GE Bio-Sciences, Piscataway, NJ) and eluted with Q2 buffer. Fractions with ClpP were combined and dialyzed against Clp buffer at 4°C and stored at -80°C.

Filamin

The multidomain substrate was constructed in pFN18A (Promega) which encoded a mutant version of the *Rhodococcus rhodochrous* haloalkane dehalogenase (HaloTag) domain at the N terminus [33], a linker of 47 residues containing two TEV protease sites, immunoglobulin repeats 1–8 of human filamin, residues 5303–5341 of human Filamin A, a His₆ tag, and a C-terminal AANDENYALAA ssrA tag. This substrate was expressed in *E. coli* strain ERL [15]. Filamin was expressed in LB with carbenicillin (50 µg/ml) and kanamycin (30 µg/mL) with 1 mM IPTG during 4 hrs at 25°C. The lysis

protocol was the same used for ClpX but buffer W was used for washing and E buffer for elution of protein from the Ni²⁺-NTA affinity column (QIAGEN). Samples containing protein were combined and loaded onto a Superdex 200HRcolumn (GE Bio-Sciences, Piscataway, NJ) and purified following the same protocol used for ClpX.

Protease Assays

Filamin substrate was incubated with aliquots of ClpP (440 nM) and ClpX (110 nM) in the presence of 20 mM ATP. The reaction mixture (60–100 µL), if necessary, was incubated at 22°C or 37°C for different times. All reactions were stopped on liquid nitrogen by the addition of SDS-PAGE loading buffer followed by a heating step at 100°C for 10 min. After centrifugation at 14,000 rpm in a table centrifuge during 10 min, samples were loaded into a SDS-page electrophoresis gel. For visualizing filamin and byproducts after degradation by ClpXP, filamin was pre-mixed with 1 µM of HaloTag Coumarin Ligand (Promega) and PD buffer was used for the degradation reaction. Proteins in the fractions were observed by staining with Coomassie Blue after SDS-polyacrylamide gel electrophoresis; 25 µL of each reaction was applied to the different lanes. Polyacrylamide gel electrophoresis (PAGE) in the presence of sodium dodecylsulfate (SDS) was performed in 10% gels which were then stained with Coomassie Blue. The reduced samples were treated with 2% 2-mercaptoethanol and boiled for 10 min.

Preparation of HaloTag ligand cover slips for AFM

The glass surface was cleaned with Hellmanex overnight, and after washing extensively it was plasma-cleaned, and then silanized with (3-Aminopropyl)triethoxysilane (Sigma) by the gas phase method. All chemical modification and incubations were performed at room temperature. After silanization, the glass was reacted for 1 h with 25 mM succinimidyl-[(N-maleimidopropionamido)-tetracosaehtylene glycol] ester (SM-(PEG)24, Thermo Fisher Scientific, Waltham, MA) in Borax buffer (pH 8.5), in the dark. After washing with double distilled water the surface was incubated for at least 1h in 30 mM HaloTag ligand thiol (O4) (Promega) in Borax buffer and the reaction was quenched with 30 mM 1-propanethiol (Sigma) for 10 min and washed with double-distilled water. Finally the HaloTag-Filamin was added to the surface and left to adsorb for 10 min.

Preparation of streptavidin cover slips

Glass cover slips were covered with 3-aminopropyl dimethyl ethoxysilane during 2 hrs. The surface was washed with borax buffer during 1 hr and covered with BB buffer during 1 hr at room temperature. The cover slides were washed with Borax buffer and Streptavidin

buffer was added during 1 hr at 4°C. Finally, the slides were washed with PB buffer and stored at -20°C.

Preparation of HaloTag Beads

Magnetic amine functionalized beads were mixed with SM(PEG)24 (Thermo Scientific) in 250 mM of DMSO at room temperature for 1 hr. After this, 2 µL of HaloTag Ligand (Promega) were combined with the beads and 12 µL of Filamin (HaloTag-FLN₈-ssrA) were added. This reaction was conducted for 1 hr at 4°C and was followed by the addition of 1 µL of ethanolamine and 1 µL of ethanethiol for 10 min to block any unreacted groups on the surface of the beads.

Degradation and Denaturation Assays

Magnetic tweezers experiments were conducted using a set-up under force-clamp conditions as described in [19].

ACKNOWLEDGEMENTS

I thank Dr. J. Fernandez for allowing me to participate in this most important research. The technical skillful assistance of Dr C. Badilla, Dr. I. Popa and Dr. J. Alegre-Cebollada is gratefully acknowledged.

1. Gottesman, S. and M.R. Maurizi, *Regulation by proteolysis: energy-dependent proteases and their targets*. Microbiol Rev, 1992. **56**(4): p. 592-621.
2. Hargrove, J.L. and F.H. Schmidt, *The role of mRNA and protein stability in gene expression*. FASEB J, 1989. **3**(12): p. 2360-70.
3. Knecht, E., et al., *Intracellular protein degradation in mammalian cells: recent developments*. Cell Mol Life Sci, 2009. **66**(15): p. 2427-43.
4. Christiaens, V., I. Scroyen, and H.R. Lijnen, *Role of proteolysis in development of murine adipose tissue*. Thromb Haemost, 2008. **99**(2): p. 290-4.
5. Maurizi, M.R., et al., *Sequence and structure of Clp P, the proteolytic component of the ATP-dependent Clp protease of Escherichia coli*. J Biol Chem, 1990. **265**(21): p. 12536-45.
6. Yu, A.Y. and W.A. Houry, *ClpP: a distinctive family of cylindrical energy-dependent serine proteases*. FEBS Lett, 2007. **581**(19): p. 3749-57.
7. Katayama-Fujimura, Y., S. Gottesman, and M.R. Maurizi, *A multiple-component, ATP-dependent protease from Escherichia coli*. J Biol Chem, 1987. **262**(10): p. 4477-85.
8. Wang, J., J.A. Hartling, and J.M. Flanagan, *The structure of ClpP at 2.3 Å resolution suggests a model for ATP-dependent proteolysis*. Cell, 1997. **91**(4): p. 447-56.
9. Olinares, P.D., J. Kim, and K.J. van Wijk, *The Clp protease system; a central component of the chloroplast protease network*. Biochim Biophys Acta, 2011. **1807**(8): p. 999-1011.
10. Beuron, F., et al., *At sixes and sevens: characterization of the symmetry mismatch of the ClpAP chaperone-assisted protease*. J Struct Biol, 1998. **123**(3): p. 248-59.
11. Grimaud, R., et al., *Enzymatic and structural similarities between the Escherichia coli ATP-dependent proteases, ClpXP and ClpAP*. J Biol Chem, 1998. **273**(20): p. 12476-81.
12. Glynn, S.E., et al., *Structures of asymmetric ClpX hexamers reveal nucleotide-dependent motions in a AAA+ protein-unfolding machine*. Cell, 2009. **139**(4): p. 744-56.
13. Kim, Y.I., et al., *Dynamics of substrate denaturation and translocation by the ClpXP degradation machine*. Mol Cell, 2000. **5**(4): p. 639-48.
14. Baker, T.A. and R.T. Sauer, *ClpXP, an ATP-powered unfolding and protein-degradation machine*. Biochim Biophys Acta, 2011.
15. Aubin-Tam, M.E., et al., *Single-molecule protein unfolding and translocation by an ATP-fueled proteolytic machine*. Cell, 2011. **145**(2): p. 257-67.
16. Joshi, S.A., et al., *Communication between ClpX and ClpP during substrate processing and degradation*. Nat Struct Mol Biol, 2004. **11**(5): p. 404-11.
17. Barkow, S.R., et al., *Polypeptide translocation by the AAA+ ClpXP protease machine*. Chem Biol, 2009. **16**(6): p. 605-12.
18. Davis, J.H., T.A. Baker, and R.T. Sauer, *Engineering synthetic adaptors and substrates for controlled ClpXP degradation*. J Biol Chem, 2009. **284**(33): p. 21848-55.
19. Liu, R., et al., *Mechanical characterization of protein L in the low-force regime by electromagnetic tweezers/evanescent nanometry*. Biophys J, 2009. **96**(9): p. 3810-21.
20. Neuman, K.C. and A. Nagy, *Single-molecule force spectroscopy: optical tweezers, magnetic tweezers and atomic force microscopy*. Nat Methods, 2008. **5**(6): p. 491-505.
21. Los, G.V., et al., *HaloTag: a novel protein labeling technology for cell imaging and protein analysis*. ACS Chem Biol, 2008. **3**(6): p. 373-82.
22. Lang, C., et al., *HaloTag: a new versatile reporter gene system in plant cells*. J Exp Bot, 2006. **57**(12): p. 2985-92.
23. Wang, K., *Filamin, a new high-molecular-weight protein found in smooth muscle and nonmuscle*

- cells. *Purification and properties of chicken gizzard filamin*. *Biochemistry*, 1977. **16**(9): p. 1857-65.
24. Wallach, D., P.J. Davies, and I. Pastan, *Purification of mammalian filamin. Similarity to high molecular weight actin-binding protein in macrophages, platelets, fibroblasts, and other tissues*. *J Biol Chem*, 1978. **253**(9): p. 3228-35.
25. Zhou, A.X., J.H. Hartwig, and L.M. Akyurek, *Filamins in cell signaling, transcription and organ development*. *Trends Cell Biol*, 2010. **20**(2): p. 113-23.
26. Stossel, T.P., et al., *Filamins as integrators of cell mechanics and signalling*. *Nat Rev Mol Cell Biol*, 2001. **2**(2): p. 138-145.
27. Furuike, S., T. Ito, and M. Yamazaki, *Mechanical unfolding of single filamin A (ABP-280) molecules detected by atomic force microscopy*. *FEBS Lett*, 2001. **498**(1): p. 72-5.
28. Kenniston, J.A., T.A. Baker, and R.T. Sauer, *Partitioning between unfolding and release of native domains during ClpXP degradation determines substrate selectivity and partial processing*. *Proc Natl Acad Sci U S A*, 2005. **102**(5): p. 1390-5.
29. Maillard, R.A., et al., *ClpX(P) generates mechanical force to unfold and translocate its protein substrates*. *Cell*, 2011. **145**(3): p. 459-69.
30. Martin, A., T.A. Baker, and R.T. Sauer, *Rebuilt AAA + motors reveal operating principles for ATP-fuelled machines*. *Nature*, 2005. **437**(7062): p. 1115-20.
31. Shin, Y., et al., *Single-molecule denaturation and degradation of proteins by the AAA+ ClpXP protease*. *Proc Natl Acad Sci U S A*, 2009. **106**(46): p. 19340-5.
32. Chen, I., et al., *Site-specific labeling of cell surface proteins with biophysical probes using biotin ligase*. *Nat Methods*, 2005. **2**(2): p. 99-104.
33. Los, G.V. and K. Wood, *The HaloTag: a novel technology for cell imaging and protein analysis*. *Methods Mol Biol*, 2007. **356**: p. 195-208.

SUPPLEMENTAL MATERIAL

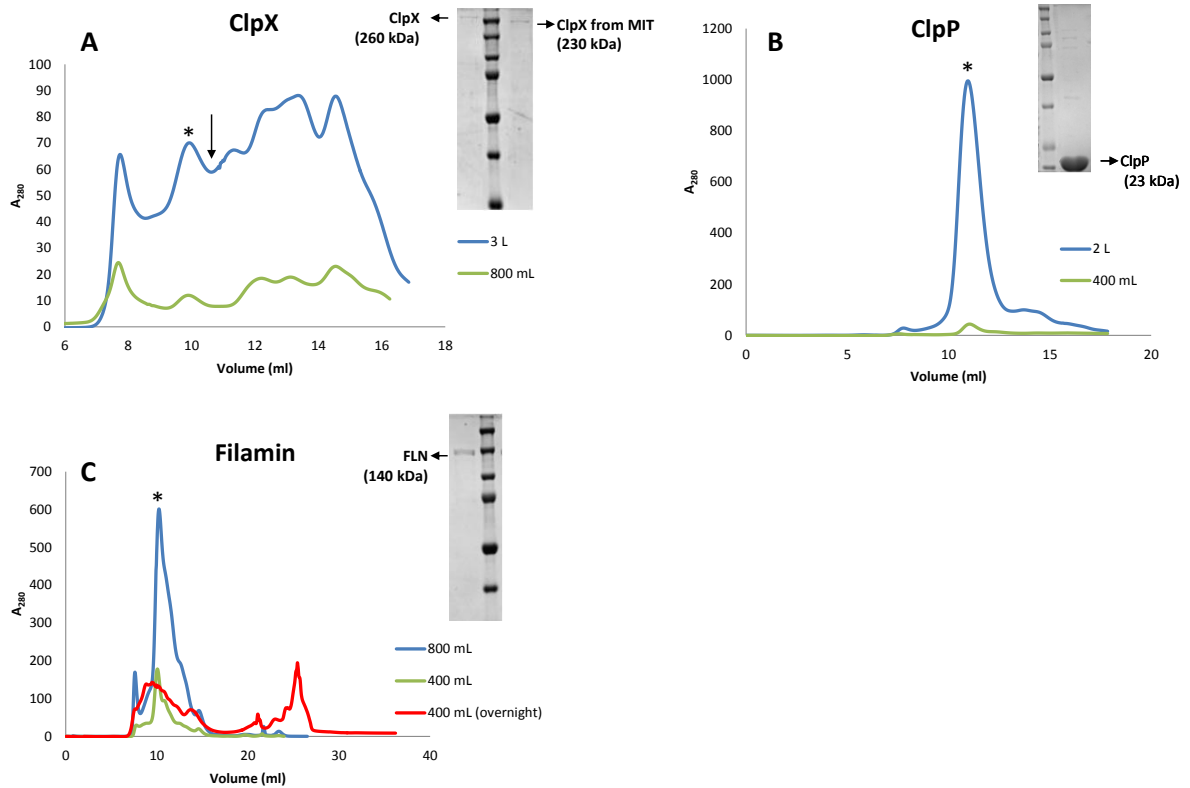


Fig 1. Purification of ClpX, ClpP and Filamin on Superdex 200HR column . The protein-containing fractions from the metal affinity column were pooled and run over a Superdex 200HR column. The proteins eluted with the appropriate buffer were monitored by absorbance at 280 nm (solid line), and 250 μ L aliquots were collected. The main fraction of each protein is represented by an asterisk and it was analyzed by SDS-PAGE (contiguous gel in each figure). **A:** The green line represents a purification of ClpX using 800 mL of cell culture which resulted in a very low concentration of protein (second peak). The green line represents a second attempt for ClpX purification (second peak) using 2 L of cell culture and Ammonium sulfate to concentrate the protein. The arrow shows the position where the peak of ClpX should appear. **B:** ClpP purification using 2 L (blue line) or 400 mL of culture (green line). **C:** Each line shows the results of the purification of filamin following different protocols. Blue line and green line represent the results of filamin purification as described in Methods, employing 800 mL and 400 mL of cell culture respectively. The red line represents the results obtained from the same protocol described in Methods, but expressing filamin overnight.

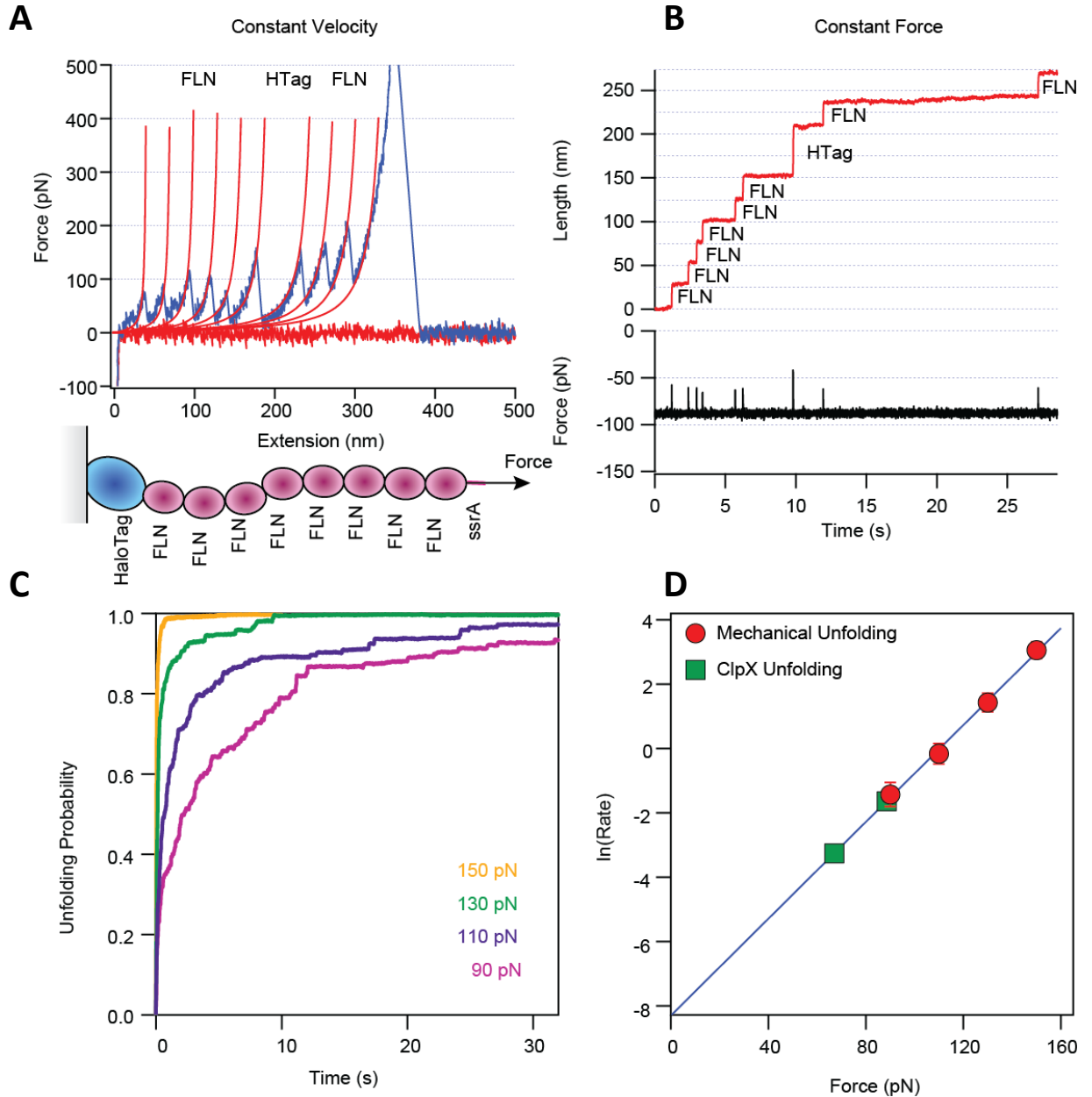


Figure 2. Study of the extension of Filamin. **A** When filamin is pulled at constant velocity the pulling force initiates the unfolding of a FLN module or the HaloTag protein. In this case, there are nine peaks corresponding to the unfolding of eight FLN modules and the HaloTag protein. The contour length of the FLN domains is 32 nm and of the HaloTag of 66 nm, in accordance with their number of aminoacids released to force after mechanical unfolding. **B** When pulling is done under a feedback system that maintains the force constant, a stair-like elongation is observed composed by nine steps. **C**. Unfolding probability increases with higher forces. **D**. Comparison of the force-dependent rate during mechanical unfolding (AFM) and ClpX unfolding [15].

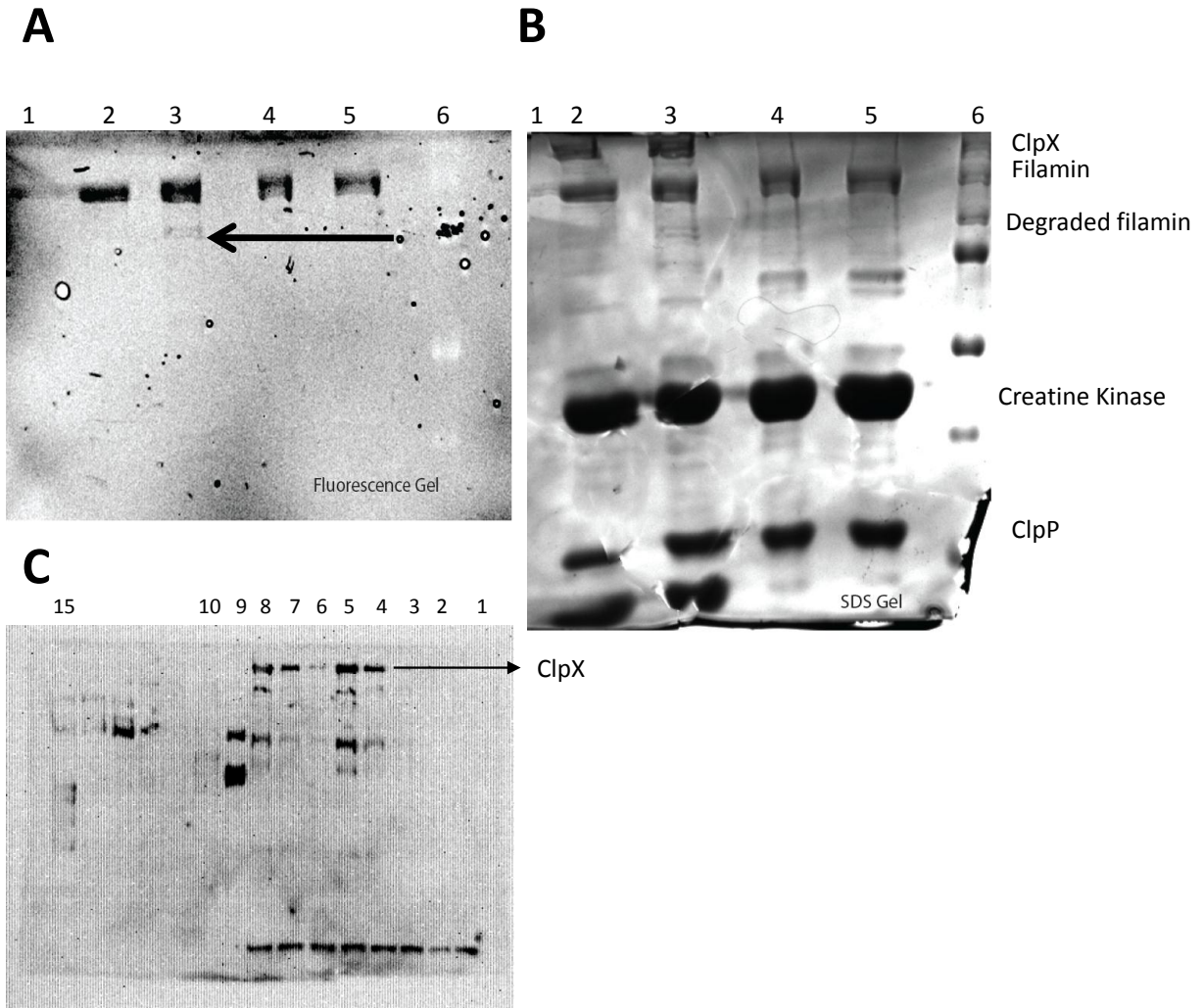


Figure 3. Protease activity analyzed by SDS-polyacrylamide (10%) gel electrophoresis. A: Bands observed under irradiation of UV light ($\lambda=590$ nm). Lanes 1 and 3: Reaction of Filamin and ClpXP during 15 seconds. Lanes 2 and 4: Reaction of Filamin and ClpXP during 10 minutes. The arrow shows a fragment of product of filamin degradation by ClpXP. **B:** Same gel observed in figure 3A but the bands were stained with Coomassie Blue **E:** Lane 1: Reaction of filamin and ClpXP overnight at 37°C. Lane 2: Filamin alone. Lane 3: ClpP alone. Lane 4: ClpX alone. Lane 5: ClpXP. Lane 6: ClpXP plus ATP. Lane 7: ATP. Lane 8: Reaction of Filamin, ClpXP at 22°C during 10 min. **C.** Pilot expression of ClpX changing the time of expression. Each sample was subjected to western blotting with an antibody against His-tag. Lane 1: Non induced sample. Lane 2: Sample induced for 2 hrs. Lane 3 and 6: Sample induced for 3 hrs. Lane 4 and 7: Sample induced for 4 hrs. Lane 5 and 8: Sample induced overnight. Lane 9: Molecular marker. Lanes 10 to 15: Main fractions of the purification showed in figure 1A using 2 L of cell culture.

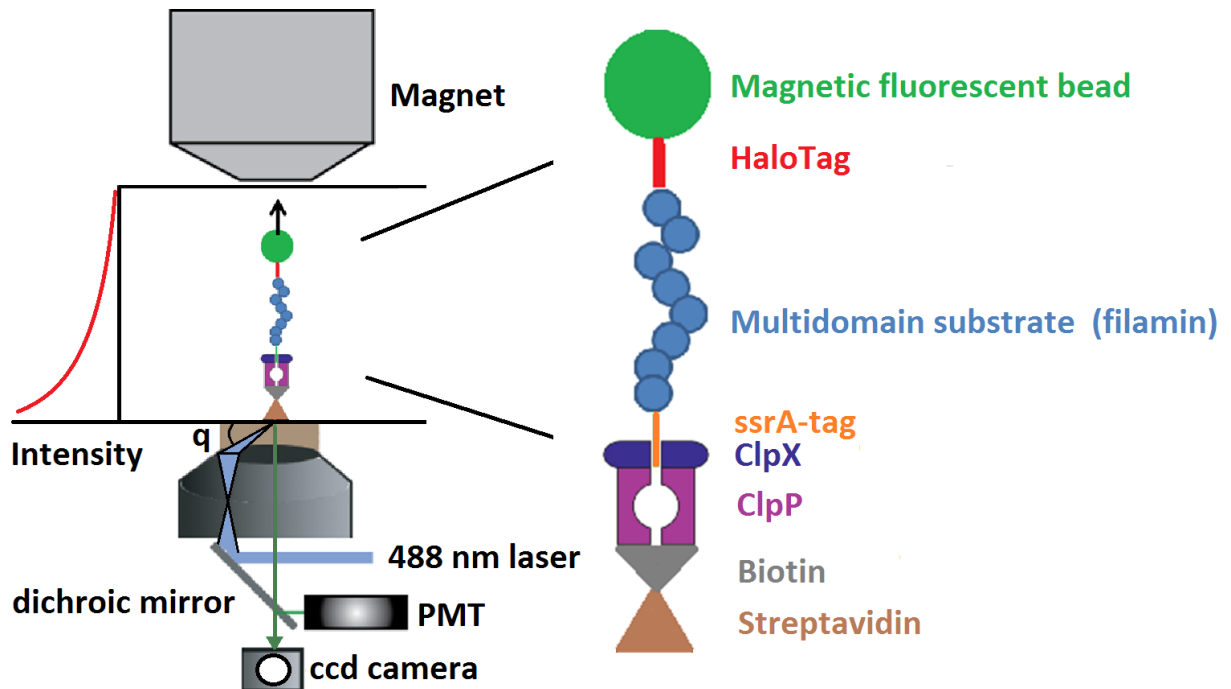


Figure 4. Representation of the experimental set-up based on magnetic tweezers to analyze the mechanical properties of ClpXP. ClpXP was tethered to the glass cover slip by biotin-streptavidin interaction; a multidomain protein was attached to a magnetic fluorescent bead by the covalent union of the HaloTag, and connectivity between the glass cover slip and the bead was maintained by interaction between ClpXP and filamin. The extension of the polyprotein is measured from the fluorescence intensity of the fluorescent bead within a vanishing TIRF field.

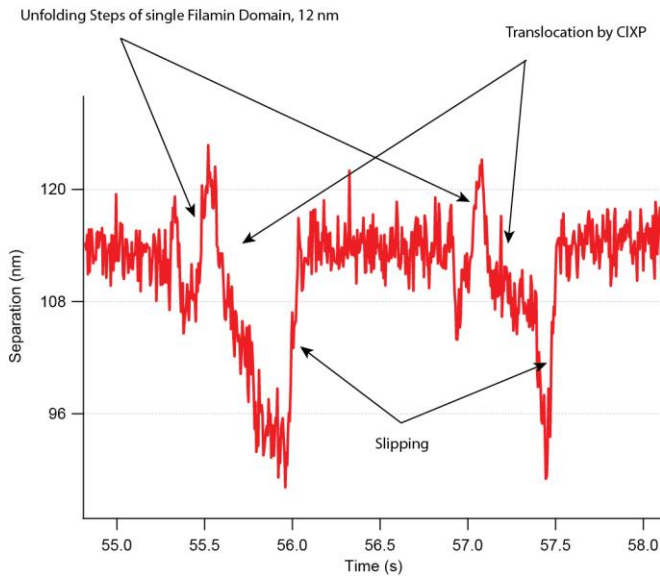


Fig 5. Separation-versus-time trace of unfolding and translocation events, accompanying slipping of the substrate and non-degradation of the multidomain substrate.

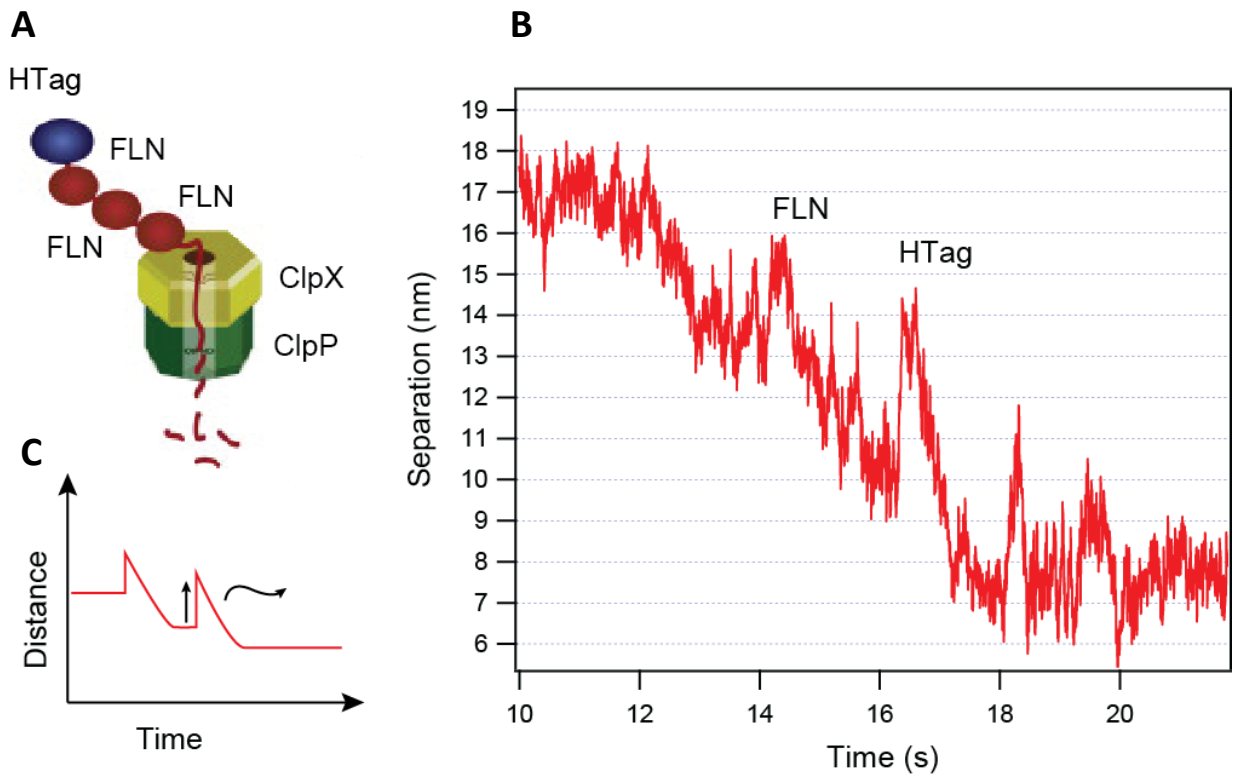


Figure 6. Model of the mechanical unfolding of the multidomain substrate by ClpXP. A: Representation of the ClpXP protease degrading a multidomain substrate. **B:** Separation-versus-time trace of unfolding and translocation events followed by ClpXP degradation of the multidomain substrate **C:** Expected result of ClpXP activity: Unfolding a domain of the substrate results in an increase in the bead-glass distance, whereas translocation of the unfolded peptide decreases the distance. Each dwell is the time necessary to unfold the next domain.